Bioconjugate Chemistry

Article

pubs.acs.org/bc

Oligonucleotides Conjugated to Natural Lipids: Synthesis of Phosphatidyl-Anchored Antisense Oligonucleotides

Rosa Chillemi,[†] Valentina Greco,*[,‡] Vincenzo G. Nicoletti,[†] and Sebastiano Sciuto[†]

[†]Dipartimento di Scienze Chimiche, Università di Catania, V. le A. Doria 6, 95125 Catania, Italy

[‡]Istituto di Biostrutture e Bioimmagini, Consiglio Nazionale delle Ricerche, V. le A. Doria 6, 95125 Catania, Italy

Supporting Information

ABSTRACT: Antisense oligonucleotides are promising therapeutic agents against a variety of diseases. Effective delivery of these molecules is critical in view of their clinical application. Despite the richness of synthetic strategies addressed to the lipophilic modification of oligodeoxynucleotides (ODNs) for enhancing their pharmacokinetic behavior and trans-membrane delivery, the phosphatidyl group (1,2-di-*O*-acyl-*sn*-glycero-3-phosphoryl) has been never used as the lipophilic moiety of lipid−ODN conjugates. The present paper reports a general procedure for synthesizing 5′-phosphatidyl-ODNs. By this procedure, phosphatidyl conjugates of a VEGF antisense-ODN have been prepared, which differ in the fatty acid composition of their phosphatidyl moiety. These new lipid−ODN conjugates, which have been characterized on the basis of their physicochemical properties, showed an improved resistance to exonucleases and were able to lower the VEGF-mRNA expression in human SH-SY5Y neuroblastoma cells more effectively than the relevant free antisense−ODN did.

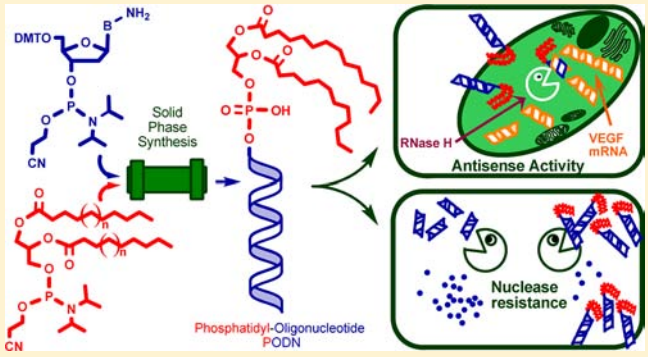

INTRODUCTION

Over the past two decades, antisense oligonucleotides (ASONs) have emerged as valuable tools for functional genomics, gene target validation, and therapeutic purposes. However, one major barrier in the broad utilization of ASONs is their reduced ability to cross cell membranes.[1,2] However, cellular uptake and localization of ASONs are crucial problems for their effects on the genetic expressions.

With the aim of improving cellular uptake and antisense activity, single-stranded oligodeoxynucleotides (ODNs) have been tethered to numerous lipophilic moieties including the widely used cholesterol,[3−6,8] alkyl chain,[7−9] di-*O*-alkyl-*rac*-glycerol,[7,8,10] and adamantane.[7,8] More recently, in order to address the same problem, short interfering RNAs have also been modified by conjugating them with cholesterol, lithocholic acid, and 12-hydroxylauric acid as well.[11]

It goes without saying that pharmacologically active oligonucleotides bearing biocompatible lipophilic groups, attached possibly through a phosphoester bond, would be useful pro-drugs with improved cellular uptake. However, despite the richness of the synthetic strategies developed for the modification of the ODNs,[12] the synthesis of lipid−ODN conjugates is anything but trivial and requires extensive expertise in organic chemistry and solid-phase synthesis. A prime example in this regard relates the case of the phosphatidyl group. This latter, on account of its widespread occurrence in the molecular structures of many lipid constituents of cell membranes, would be one of the most appropriate lipophilic groups to bind to ODNs. This is also consistent with previous reports where cholesterol or single alkyl tail oligonucleotide or polysaccharide conjugates have shown lower insertion levels in membranes than two-chain lipid tail conjugates.[13−15]

Nevertheless, although various synthetic strategies have been addressed to the lipophilic modification of ODNs,[16] phosphatidyl group (1,2-di-*O*-acyl-*sn*-glycero-3-phosphoryl) has been never used as the lipophilic moiety of lipid−ODN conjugates. This essentially depends on an actual difficulty encountered in a direct attachment of these groups to ODNs elongated on solid phase by standard phosphoramidite chemistry procedures; such a way, in fact, suffers from the lability of the carboester bond in these groups under the strongly basic conditions routinely used to remove classical amino protecting groups of nucleotides.

Some years ago, aiming to overcome the above drawbacks, we considered the possibility of preparing phosphatidyl-like conjugates of oligonucleotides[17] by exploiting a two-step chemoenzymatic strategy we had previously developed for preparing lipid-conjugates of deoxyribo- and ribonucleosides as well.[18] So, 5′-*O*-glycerophosphoryloligonucleotides (5′-GPODNs) were first prepared on solid phase by phosphoramidite chemistry and, in a subsequent step, acylation at the

Received: November 12, 2012
Revised: February 11, 2013
Published: March 1, 2013

   dx.doi.org/10.1021/bc300602g | *Bioconjugate Chem.* 2013, 24, 648−657

glycerol moiety was performed in organic solvent by a lipase-catalyzed transacylation with activated fatty acid esters. Although some short-chain lysophosphatidyloligonucleotides (but not the phosphatidyl ones) were actually prepared by this route, the extension of the synthetic method to prepare this kind of lipid−ODNs longer than 6-mer was impracticable.[17]

In the early 2000s, an efficient solid-phase synthesis of oligodeoxynucleotides was reported[19,20] that made use of *N*-unprotected nucleoside phosphoramidites and 1-hydroxybenzotriazole (HOBt) as promoter for the activation of each of the phosphoramidite building blocks. This procedure, called "activated phosphite method", is based on formation of bulky phosphite-type intermediates which would not react with free amino groups of nucleobases. By the combined use of the "activated phosphite method" and new silyl-type linkers, that could be cleaved under neutral conditions, the authors synthesized oligonucleotides incorporating alkali-labile modified bases, such as N^4-acetylcytosine.[19]

Now, taking advantage of these synthetic opportunities and making the appropriate changes, we developed a general synthetic pathway that allows the preparation of phosphatidyl conjugates of oligodeoxynucleotides (PODNs) which may be different in the fatty acid composition of their phosphatidyl moiety and in the oligonucleotide base-sequence as well.

EXPERIMENTAL PROCEDURES

Materials and Methods. All solvents and reagents employed in the syntheses were reagent grade, the majority of which were purchased from either Sigma-Aldrich or Fluka. 1,2-Di-*O*-myristoyl-*sn*-glycerol, 1,2-di-*O*-palmitoyl-*sn*-glycerol, and 1,2-di-*O*-stearoyl-*sn*-glycerol were purchased from Bachem. 5′-*O*-(4,4′-Dimethoxytrityl)-thymidine-3′-[(2-cyanoethyl)-*N*,*N*-diisopropyl]-phosphoramidite, 5′-*O*-(4,4′-dimethoxytrityl)-N^6-benzoyl-2′-deoxyadenosine-3′-[(2-cyanoethyl)-*N*,*N*-diisopropyl)-phosphoramidite, 5′-*O*-(4,4′-dimethoxytrityl)-N^4-benzoyl-2′-deoxycytidine-3′-[(2-cyanoethyl)-*N*,*N*-diisopropyl]-phosphoramidite, 5′-*O*-(4,4′-dimethoxytrityl)-N^2-isobutyryl-2′-deoxyguanosine-3′-[(2-cyanoethyl)-*N*,*N*-diisopropyl]-phosphoramidite, Amidite Diluent, Activator, Cap A, Cap B, Deblocking and Oxidizing solutions, as well as Glen-Pak DNA Purification Cartridge 3 g were all from Glen Research. Solid CO_2 was freshly prepared following gas expansion. TLC was carried out on silica gel 60 F_{254} plates (Merck); the spots were visualized by UV light (λ = 254 nm) or by spraying the plates with Rhodamine B reagent. PLC was performed on silica gel (63−200 μm, Merck). HPLC was performed on a Varian 9010 chromatograph equipped with a UV−vis detector set at λ = 260 nm. Solid-phase synthesis of either modified or unmodified oligonucleotides was carried out on automated DNA synthesizer Cyclone Plus 8400 (Biosearch). ^{1}H and ^{13}C NMR spectra were recorded on a Varian Unity Inova spectrometer at 500 and 125.7 MHz, respectively. The chemical shifts are reported as δ (ppm) and referenced to the TMS resonance, for the experiments in $CDCl_3$ and CD_3OD and to the resonance of residual HOD for ^{1}H experiments in D_2O. HPLC-ESI/MS was carried out on Agilent Technologies 6410 Triple Quad LC/MS equipped with Agilent Multimode (ESI/APCI) source. UV spectra were recorded on JASCO V-560 UV/vis spectrometer using 1 cm path length quartz cuvettes.

When required, solvents were freshly dried and stored on molecular sieves 3 Å type (Fluka). Before use, 1-hydroxybenzotriazole·$x$$H_2O$ (HOBt, Fluka) was allowed to stand under reduced pressure over P_2O_5 at rt for 48 h. Care must be taken not to dry HOBt out completely or it may cause an explosion.

Synthesis of 3′-*O*-{Diisopropyl[4-(2,4,6-tribromophenoxycarbonyl)phenyl]silyl}-5′-*O*-(4,4′-dimethoxytrityl)-thymidine (2). The title synthesis was accomplished following a previously reported procedure.[21] ^{1}H NMR spectrum of the intermediate 2,4,6-tribromophenyl 4-(diisopropylsilyl)benzoate (**1**) and that of compound **2**, which are not reported in the cited literature, are given in the Supporting Information.

Anchoring of Compound 2 to LCAA-CPG. The synthetic step referred to in title was performed by slightly modifying a previously reported procedure.[21] LCAA-CPG (1.22 g; loading capacity 136 μmol/g), compound **2** (362 mg ; 332 μmol), and 47 μL (332 μmol) of dry TEA were suspended in dry CH_2Cl_2/DMF (1:1 v/v) and left under stirring for 36 h. After this period, the suspension was introduced in an empty reaction column of those commonly used in automated synthesizers, and the solid phase trapped in the column was successively washed with CH_2Cl_2, THF, and ACN (all dry). Capping of unreacted amino groups was then achieved by flushing into the column a solution containing 30 mM Ac_2O and 60 mM DMAP in 10 mL of THF, and allowing to stand for 2.5 h. Finally, the column was washed with 20 mL of CH_2Cl_2 and 20 mL of THF (all dry).

After the siliceous support **3** was dried, an aliquot was treated with a solution of 2.5% $CHCl_2COOH$ in CH_2Cl_2 and the released dimethoxytrityl groups were spectrophotometrically quantified. The loading capacity was 30.6 μmol/g.

***N*-Unprotected 5′-*O*-(4,4′-Dimethoxytrityl)-2′-deoxynucleoside-3′-[(2-cyanoethyl)-*N*,*N*-diisopropyl]-phosphoramidites.** The title compounds were prepared by treating the commercially available 5′-*O*-(4,4′-dimethoxytrityl)-N^6-benzoyl-2′-deoxyadenosine-3′-[(2-cyanoethyl)-*N*,*N*-diisopropyl]-phosphoramidite, 5′-*O*-(4,4′-dimethoxytrityl)-N^4-benzoyl-2′-deoxycytidine-3′-[(2-cyanoethyl)-*N*,*N*-diisopropyl]-phosphoramidite, and 5′-*O*-(4,4′-dimethoxytrityl)-N^2-isobutyryl-2′-deoxyguanosine-3′-[(2-cyanoethyl)-*N*,*N*-diisopropyl]-phosphoramidite with 2 M $MeNH_2$ in anhydrous THF. ^{1}H NMR spectra of each unprotected nucleoside phosphoramidite were in accordance with literature data.[22]

General Procedure for the Synthesis of 1,2-Di-*O*-acyl-*sn*-glycero-3-[(2-cyanoethyl)-*N*,*N*-diisopropyl]-phosphoramidites (7−9). To a solution of the appropriate 1,2-di-*O*-acyl-*sn*-glycerol (**4**−**6**; 1 mmol) in 15 mL of anhydrous CH_2Cl_2, *N*,*N*-diisopropylethylammine (0.68 mL, 4 mmol) and 2-cyanoethyl-*N*,*N*-diisopropylchlorophosphoramidite (0.44 mL, 2 mmol) were added under Ar. The mixture was stirred for 1 h and, after addition of 20 mL of CH_2Cl_2, it was extracted with saturated aqueous $NaHCO_3$. The organic phase was dried over Na_2SO_4 and evaporated in vacuo. The residue was purified by PLC, by eluting with petroleum ether/ethyl ether/*tert*-BuOH/TEA [88:6:5:1 (v/v)]; fractions containing pure 1,2-di-*O*-acyl-*sn*-glycero-3-[(2-cyanoethyl)-*N*,*N*-diisopropyl]-phosphoramidite, detected by Rhodamine B reagent, were pooled and taken to dryness in vacuo.

1,2-Di-O-myristoyl-sn-glycero-3-[(2-cyanoethyl)-N,N-diisopropyl]-phosphoramidite (7). Compound **7** was obtained starting from 1,2-di-*O*-myristoyl-*sn*-glycerol (**4**); 87% yield as mixture of the two expected diastereomers; ^{1}H NMR ($CDCl_3$): δ 5.15 (m, 1 H, H-2 of glycerol), 4.33 and 4.28 (double doublets, $J_{1a,1b}$ = −11.5, $J_{1a,2}$ = 4.0 Hz; 1 H altogether, H-1a of glycerol), 4.136 and 4.107 (double doublets, $J_{1b,1a}$ = −11.5, $J_{1b,2}$

dx.doi.org/10.1021/bc300602g | *Bioconjugate Chem.* 2013, 24, 648−657

= 6.0 Hz, 1 H altogether, H-1b of glycerol), 3.84−3.62 (partially overlapped multiplets, 4 H, H-3a and H-3b of glycerol, OCH_2CH_2CN), 3.61−3.52 [multiplets, 2 H, $CH(CH_3)_2$], 2.587 and 2.569 (t, J = 6.5 Hz, 2 H altogether, OCH_2CH_2CN), 2.267 and 2.256 (multiplets, 4 H altogether, α-CH_2), 1.578 and 1.565 (multiplets, 4 H altogether, β-CH_2 of myristoyls), 1.25 and 1.22 (br singlets, 40 H altogether, from γ- to μ-CH_2 of myristoyls), 1.156 and 1.131 [doublets, J = 6.7 Hz, 12 H altogether, $CH(CH_3)_2$], 0.84 (t, J = 7.0 Hz, 6 H, CH_3 of myristoyls). ^{13}C NMR ($CDCl_3$): δ 172.93 (COO), 172.56 (COO), 117.51 and 117.22 (CN), 70.45 and 70.40 (doublets, J_{CCOP} = 6.5 Hz, C-2 of glycerol), 62.09 (C-1 of glycerol), 61.51 and 61.37 (doublets, J_{COP} = 17.2 Hz, C-3 of glycerol), 58.32 and 58.24 (partially overlapped doublets, J_{COP} = 18.7 Hz, OCH_2CH_2CN), 42.93 and 42.88 [partially overlapped doublets, J_{CNP} = 12.1 Hz, $CH(CH_3)_2$], 34.04 and 33.84 (α-CH_2 of myristoyls), 31.69 (λ-CH_2 of myristoyls), 29.42, 29.39, 29.25, 29.11, 29.06, and 28.88 (from γ- to κ-CH_2 of myristoyls), 24.68 and 24.65 (β-CH_2 of myristoyls), 24.31 and 23.89 [doublets, J_{CCNP} = 6.8 and 7.4 Hz, respectively, $CH(CH_3)_2$], 22.44 (μ-CH_2 of myristoyls), 20.11 (d, J_{CCOP} = 6.8 Hz, OCH_2CH_2CN), 13.84 (CH_3 of myristoyls). ESI-MS(+) m/z: Calc. for $C_{40}H_{78}N_2O_6P^+$: 713.56 $[M + H]^+$. Found: 713.5 $[M + H]^+$, 735.5 $[M + Na]^+$, 751.5 $[M + K]^+$.

*1,2-Di-O-palmitoyl-sn-glycero-3-[(2-cyanoethyl)-N,N-diisopropyl]-phosphoramidite (**8**).* Compound **8** was obtained starting from 1,2-di-*O*-palmitoyl-*sn*-glycerol (**5**); 85% yield as mixture of the two expected diastereomers; ESI-MS(+) m/z: Calc. for $C_{44}H_{86}N_2O_6P^+$: 769.62 $[M + H]^+$. Found: 769.6 $[M + H]^+$, 791.5 $[M + Na]^+$, 807.5 $[M + K]^+$.

*1,2-Di-O-stearoyl-sn-glycero-3-[(2-cyanoethyl)-N,N-diisopropyl]phosphoramidite (**9**).* Compound **9** was obtained starting from 1,2-di-*O*-stearoyl-*sn*-glycerol (**6**); 88% yield as mixture of the two expected diastereomers; ESI-MS(+) m/z: Calc. for $C_{48}H_{94}N_2O_6P^+$: 825.68 $[M + H]^+$. Found: 825.7 $[M + H]^+$, 847.6 $[M + Na]^+$, 863.6 $[M + K]^+$.

General Procedure for the Synthesis and Purification of 5′-*O*-(1,2-Di-*O*-acyl-*sn*-glycero-3-phosphoryl)-d(TGGCTTGAAGATGT) (PODNs 10−12). The solid-phase synthesis of compounds **10**−**12** was accomplished on an automated DNA synthesizer following the phosphoramidite protocol, but using a reaction column filled with the support **3** (450 mg, 13.7 μmol loaded), a solution of 0.2 M HOBt in dry ACN/NMP 15:1 as the activator, the appropriate *N*-unprotected phosphoramidites, and, in the last coupling step, the pertinent 1,2-di-*O*-acyl-*sn*-glycero-3-[(2-cyanoethyl)-*N*,*N*-diisopropyl]-phosphoramidite (**7**−**9**; 0.1 M in dry CH_2Cl_2). In all cases, the last coupling step was repeated twice. After the synthesis was completed, the column was removed from the synthesizer, flushed slowly with 5 mL solution of 10% DBU in dry ACN, for 1 min, and then washed with dry ACN. A 3 mL solution of 1 M TBAF/AcOH (1:1) in THF was then passed repeatedly through the column by double-syringe method, going on for 1 h at 25 °C. After this period, all the TBAF/AcOH solution was recovered and the column was washed with THF (3 × 5 mL). The THF washings and the previously removed solution were then pooled and concentrated in vacuo. The residue was dissolved in ACN and charged onto a Dowex-50 × 2 (NH_4^+ form) column (10 × 130 mm) to retain TBAF excess. The column was then washed with H_2O and the eluate, taken to dryness in vacuo, was further purified by HPLC.

*HPLC Purification of PODNs **10**−**12**.* The crude compounds **10**−**12** were taken up with the minimum amount of H_2O/EtOH 1:1 (v/v) solution and submitted to HPLC analysis on Chromospher C-8 column (5 μ, 3 × 100 mm; Phenomenex) using a gradient of *i*-PrOH in 0.1 M triethylammonium acetate (pH 7.4) from 10% to 100% in 60 min, at a flow rate of 0.6 mL min^{-1}. Compounds **10**, **11**, and **12** had Rt = 31.4, 35.5, and 37.9 min, respectively. In the same chromatographic conditions, the relevant unmodified oligonucleotide had Rt = 1.21 min. Therefore, purification of compounds **10**−**12** was performed by semipreparative HPLC using Chromospher C-8 column (5 μ, 10 × 250 mm) and eluting with the same gradient of the analytical runs but using 0.1 M ammonium acetate (pH 7.4) as buffer with a flow rate of 3.5 mL min^{-1}. In each case, fractions containing the desired PODN were pooled, concentrated in vacuo to small volume, and lyophilized. PDON quantifications were then carried out in aqueous solution by means of UV-absorption analysis, using the molar extinction coefficient ε_{260} = 136 600 which was calculated by the nearest-neighbor method commonly applied to free ODN sequences.[23]

*5′-O-(1,2-Di-O-myristoyl-sn-glycero-3-phosphoryl)-d(TGGCTTGAAGATGT) (**10**).* 4.5 μmol (33% yield compared to the loading value of support **3**); ^1H NMR (D_2O, 60 °C, referenced to δ_{HOD} = 4.67 ppm) has been described in detail in Results and Discussion; compound **10**, ESI-MS(-) calcd for $C_{170}H_{230}N_{53}O_{91}P_{14}$ $(M - 3H)^{3-}$ 1635.04, found 1635.0 $[M - 3H]^{3-}$, 1225.9 $[M - 4H]^{4-}$, 980.3 $[M - 5H]^{5-}$, 816.5 $[M - 6H]^{6-}$ and 700.1 $[M - 7H]^{7-}$.

*5′-O-(1,2-Di-O-palmitoyl-sn-glycero-3-phosphoryl)-d(TGGCTTGAAGATGT) (**11**).* 3.7 μmol (27% yield compared to the loading value of support **3**); ^1H NMR spectrum of **11** was quite similar to that of compound **10** essentially differing in the integration of methylene envelope from γ- to ξ-position of palmitoyl chains (δ 1.58, 1.45, 1.32 and 1.28; 48 H altogether); compound **11**, ESI-MS(-) calcd for $C_{174}H_{238}N_{53}O_{91}P_{14}$ $(M - 3H)^{3-}$ 1653.70, found 1653.0 $[M - 3H]^{3-}$, 1240.3 $[M - 4H]^{4-}$, 992.0 $[M - 5H]^{5-}$, 826.2 $[M - 6H]^{6-}$, and 708.2 $[M - 7H]^{7-}$.

*5′-O-(1,2-Di-O-stearoyl-sn-glycero-3-phosphoryl)-d(TGGCTTGAAGATGT) (**12**).* 4.3 μmol (31% yield compared to the loading value of support **3**); also in this case, the ^1H NMR spectrum was quite similar to that of compound **10** differing in the integration of methylene envelope from γ- to π-position of stearoyl chains (δ 1.52, 1.40, 1.27, and 1.23; 56 H altogether); compound **12**, ESI-MS(-) calcd for $C_{178}H_{245}N_{53}O_{91}P_{14}$ $(M - 4H)^{4-}$ 1253.81, found 1254.0 $[M - 4H]^{4-}$, 1002.8 $[M - 5H]^{5-}$, 835.5 $[M - 6H]^{6-}$, and 716.1 $[M - 7H]^{7-}$.

Synthesis and Purification of Unmodified Sense and Antisense ODNs. Solid-phase synthesis of d(ACATCTTCAAGCCA) and d(TGGCTTGAAGATGT) was accomplished on DNA automated synthesizer by following the conventional phosphoramidite protocol. In the final synthetic step, the DMT group on 5′-terminal was retained. After the final treatment with concentrated ammonium hydroxide at rt for 1 h and then at 55 °C for 5 h, DMT-on ODNs were purified using Glen-Pak 3 g DNA Purification Cartridges and ODNs recovered, operating according to the manufacturer's manual.

Melting Temperature Measurements by DSC. DSC scans were carried out on a SETARAM micro differential scanning calorimeter (microDSC III) equipped with stainless steel 1 mL sample cells, interfaced with a Bull Micral 200 computer.

In order to obtain the excess heat capacity curves, buffer−buffer base lines were recorded at the same scanning rate and then subtracted from sample curves. Both the sample and reference cells were heated with a precision of 0.08 °C at the

Scheme 1. Outline of a Possible Synthetic Route for Solid-Phase Synthesis of 5′-*O*-Phosphatidyl Conjugates of Oligodeoxynucleotides

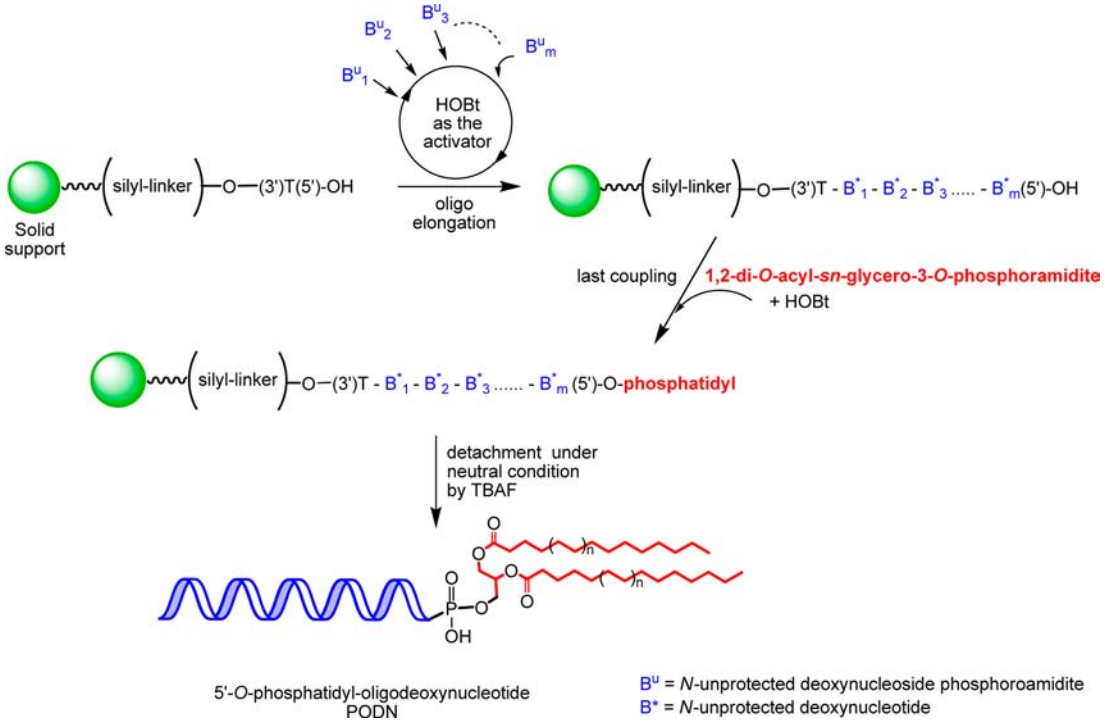

scanning rate of 1 °C min^{-1}. Calibration in energy was previously obtained by dissipating a defined power supply, electrically generated by an EJ2 SETARAM Joule calibrator within the sample cell. All DSC measurements were performed in nitrogen atmosphere.

Each oligomer which had to be annealed was dissolved in the appropriate volume of 10 mM sodium phosphate buffer (pH 7.0), containing 100 mM sodium chloride and 0.1 mM EDTA, to a final concentration of 10 μM. Immediately before the analysis, equal volumes of the sense and antisense ODN solutions or sense ODN and antisense PODN solutions were mixed together and the resulting solution was placed in the sample cell of the instrument. In a series of DSC scans, both cells were first loaded with buffer solution, equilibrated at 20 °C for 15 min, and scanned from 20 to 90 °C at a scan rate of 1 °C min^{-1}. The buffer versus buffer scan was repeated once, and upon the second cooling, the sample cell was emptied, rinsed, and loaded with the duplex solution prior to the 15 min equilibration period. Each solution sample was scanned twice to check for reversibility. The data were recorded every 2 s. The Tm value measured for the duplex from unmodified sense and antisense ODNs was 54.3 (±0.1) °C, while those measured for duplexes from sense ODN and antisense PODNs **10**, **11**, or **12** were 55.9 (±0.1), 53.2 (±0.1), and 45.2 (±0.1) °C, respectively.

Measurements of Affinity of PODNs toward a Lipid Bilayer. Supported POPC (Avanti) bilayers were prepared by adsorption and disruption of a diluted vesicular dispersion of POPC following a well-established procedure.[24] Monodisperse POPC vesicles in buffered saline (1 mM phosphate buffer, 100 mM NaCl, pH 7.4) were prepared by extrusion through polycarbonate membranes. Solutions of PODN **10**, **11**, or the unmodified ODN (all at 0.25 μM concentration) were prepared in 1 mM phosphate buffer containing 100 mM NaCl (pH 7.4). Aliquots of these solutions were injected, at a flow rate of 250 μL/min, into the measuring chamber of the Quartz Crystal Microbalance with Dissipation monitoring (QCM-D q-Sense E1) after formation of the supported lipid bilayer of POPC. All measurements were acquired at 37 °C.

Enzymatic Digestion of PODNs. Phosphodiesterase reactions were performed in parallel experiments on PODN **10**, **11**, or **12** and on the relevant unmodified ODN [0.36 $A.U._{260}$ in 0.6 mL of buffer (110 mM Tris, 15 mM $MgCl_2$, 110 mM NaCl, 30 °C)]; the buffer pH was adjusted to the desired value with HCl. Phosphodiesterase I (E.C. 3.1.4.1) from *Crotalus adamanteus* [0.5 units; Worthington Biochemicals (65 units/mg)] and each (P)ODN were incubated at pH 7.4. Incubation of phosphodiesterase II (E.C. 3.1.16.1) from bovine spleen [0.5 units; Sigma (5 units/mg)] with each (P)ODN was carried out at pH 6.5. The progress of enzymatic reactions was followed for 2 h by measuring the increase in the absorbance at 260 nm over time; absorbance values were recorded every five seconds. After the first 2 h, enzymatic reactions were allowed to proceed in the same experimental conditions for further 22 h. At the end of each total incubation period, a sample (10 μL) of the reaction mixture was analyzed by HPLC with the same procedure as reported above for the analysis of PODNs.

Reactions between PODNs **10**–**12** (3 nmol) and either phospholipase C (E.C. 3.1.4.3) from *Bacillus cereus* [4.1 units; Sigma (200 units/mg)] or phospholipase D (E.C. 3.1.4.4) from cabbage [5 units; Sigma (100 units/mg)] were conducted at 36 °C for up to 4 h in buffer (100 μL final volume, 100 mM tris, pH 8, and 10 mM $CaCl_2$). Extent of enzymatic reactions was assessed using reverse-phase HPLC as described above for the analysis of PODNs.

Biological Assays. *Evaluation of Antisense Activity.* Assays were performed by using SH-SY5Y neuroblastoma cell line cultures. The cells were maintained in Dulbecco's modified Eagle's medium (DMEM; purchased from Lonza) supplemented with 2% fetal bovine serum (FBS; Lonza) and 100 μg/

dx.doi.org/10.1021/bc300602g | *Bioconjugate Chem.* 2013, 24, 648–657

Scheme 2. Preparation of the DMT-T-Loaded LCAA-CPG (Support 3)

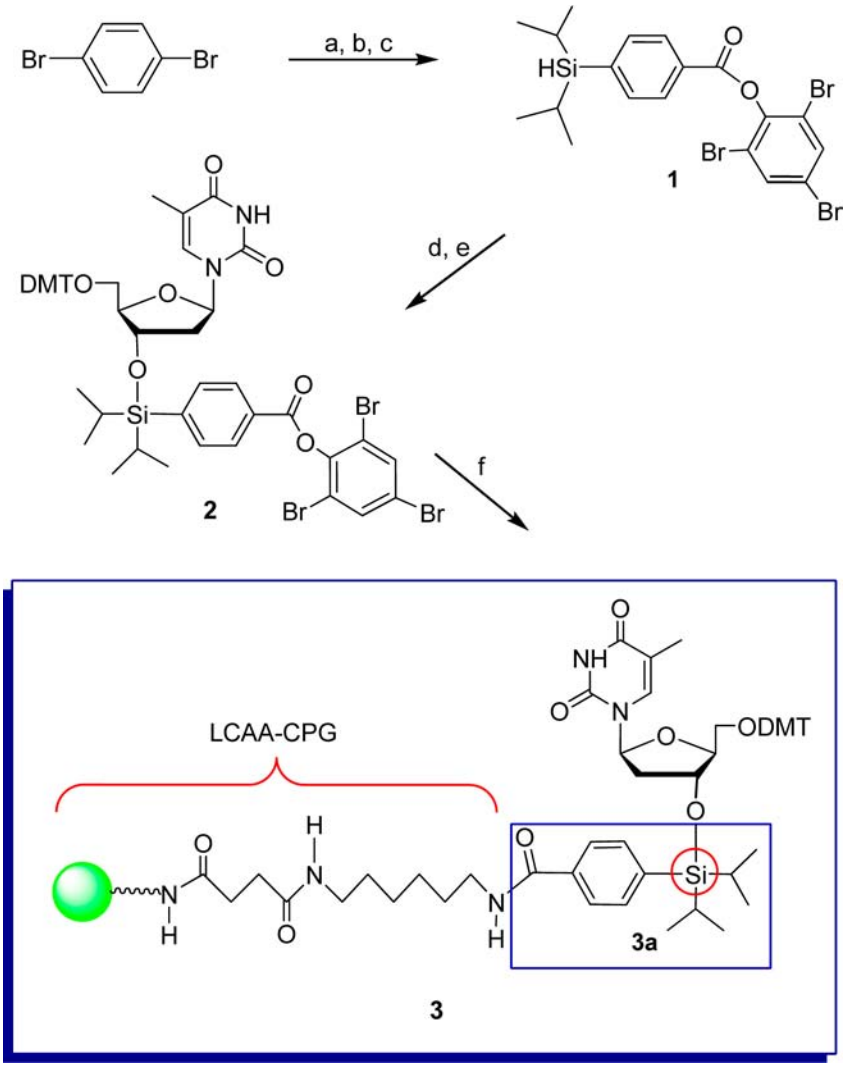

Reaction conditions: Steps (a), (b), (c), (d), and (e) were carried out according to ref 21; (f) LCAA-CPG, 0.5 equiv; 30 h, rt, CH_2Cl_2/DMF 50:50 (v/v) plus 1 equiv of Et_3N.

mL streptomycin in a humidified atmosphere of air/CO_2 (95:5) at 37 °C in an incubator (Hera Cell 150). SH-SY5Y cells were treated with PODN **10** (5, 10, and 15 μM), PODN **11** (5 and 10 μM), and the native control-ODN (10, 20, and 30 μM), also in the presence of $CoCl_2$ (25 μM). Samples of untreated cells, incubated in the above medium either with or without 25 μM $CoCl_2$, were used as control. After 60 h incubation, the growth medium was removed from culture dish and total RNA was isolated and purified using the TRIzol reagent (Invitrogen) according to manufacturer's instructions. Spectrophotometric determination of the absorbance value at 260 nm and the A_{260}/A_{280} ratio allowed us to determine the amount and purity of the isolated RNA. Total RNA (4 μg) was reverse transcribed with Superscript III First Strand kit (Invitrogen), using oligo$(dT)_{20}$ primer. Samples were incubated at 65 °C for 5 min and then at 0 °C for 1 min; afterward, 10 μL of 2× First-Strand Reaction Mix and 2 μL of Superscript III/RNase OUT Enzyme Mix (Invitrogen) were added. Samples were incubated at 50 °C for 50 min and the reaction was terminated by incubation at 85 °C for 5 min. Samples were then cooled in ice. For detection of $VEGF_{165}$ mRNA, PCR was performed by using 6.25 pmol of primers and 0.2 μL of cDNA in a reaction mixture that contained PCR buffer 5×, 50 mM $MgCl_2$, 10 mM dNTP, cDNA 40 ng, and 1 unit of Tfi DNA polymerase (Invitrogen). After an initial denaturation step at 95 °C for 5 min, 25 cycles of amplification were performed under the following conditions: 95 °C for 1 min, 55 °C for 2 min, and 72 °C for 3 min. Primers for VEGF gene amplification were as follows: Forward, 5′-ACGCTTGTTCAGAGCGGAGAA-3′, and Reverse, 5′-TAACTCAAGCTGCCTCGCCTT-3′. PCR products were analyzed by 1.0% agarose gel electrophoresis with 1× TBE buffer and visualized with SYBR (cyanine dye).

Cell Viability Tests. All the experiments were accompanied by analogous and parallel experiments aimed to assess cell viability in the various experimental conditions. This was evaluated by the MTT assay[25] after 60 h incubation. The cell count (microscopy observation, Leica DMI 4000 B) was achieved by Hoechst staining of nuclei and analyses of the captured images with the tool provided by *ImageJ* image analysis software (NIH).

dx.doi.org/10.1021/bc300602g | *Bioconjugate Chem.* 2013, 24, 648−657

RESULTS AND DISCUSSION

Synthesis and Characterization of PODNs. The general synthetic route we followed to obtain some PODNs is shown in Scheme 1. As one can easily infer from the scheme, to perform the synthesis successfully, it was necessary that, besides the first nucleoside unit anchored through a silyl-type linker to a solid support, individual *N*-unprotected nucleoside-phosphoramidites and the appropriate diacylglycerol phosphoramidite also had to be available.

Different silyl ether-type linkers have been proposed in recent literature, these being usually anchored to either siliceous (controlled pore glass, CPG) or organopolymeric (highly cross-linked polystyrene, HCP) solid supports. For our purposes we chose to anchor the 3′-OH nucleoside (thymidine) to long-chain aminoalkyl-CPG (LCAA-CPG) by 4-(diisopropylsilyl)benzoyl linker (**3a**, Scheme 2). The thymidine loaded LCAA-CPG was prepared by essentially following a previously reported method,[21] while making some small changes.

As summarized in Scheme 2, starting from 1,4-dibromobenzene, by using stepwise halogen−metal exchange reactions, the tribromophenyl ester **1** was obtained, which was first converted into the relevant silyl chloride and then allowed to react with 5′-*O*-(4,4′-dimethoxytrityl)thymidine (DMT-T) to give the active ester **2**. Reaction of **2** with LCAA-CPG gave the desired DMT-T-loaded support **3**.

The use of dichloromethane, recommended in previous work[21] as the solvent and the suspending fluid for this reaction, gave very low yield. So, it was replaced with a 1:1 (v/v) mixture of dichloromethane and dimethylformamide; this highly polar aprotic solvent, in the presence of triethylamine, was chosen to favor the nucleophilic acyl substitution reaction. The loading capacity of the obtained DMT-T-loaded support proved to be 25.6 μmol/g.

The *N*-unprotected deoxynucleoside-3′-phosphoramidite building blocks were obtained by treatment with methylamine of the relevant commercially available *N*-protected deoxynucleoside-3′-phosphoramidites, following a reported procedure.[22]

The desired 1,2-di-*O*-acyl-*sn*-glycero-3-phosphoramidites, which until now have not been reported in the literature, were prepared by reaction of **2**-cyanoethyl *N*,*N*-diisopropylchlorophosphoramidite with the pertinent diacylglycerol (Scheme 3). For this purpose, 1,2-di-*O*-tetra-, 1,2-di-*O*-hexa-, and 1,2-di-*O*-octadecanoylglycerol (**4**, **5**, and **6**, respectively) were used, all having at their chiral center the stereochemical configuration (*S*) that would have eventually provided, at the corresponding stereogenic carbon in PODNs, the absolute configuration (*R*) as that found in naturally occurring glycerophospholipids. After chromatographic purification, the individual diacylglycerophosphoramidites **7**−**9** were analyzed for their spectroscopic (^{1}H, ^{13}C NMR, and MS) properties which confirmed the expected molecular structures (see Experimental Section).

Scheme 3. Synthesis of 1,2-Di-*O*-acyl-*sn*-glycero-3-*O*-phosphoramidites

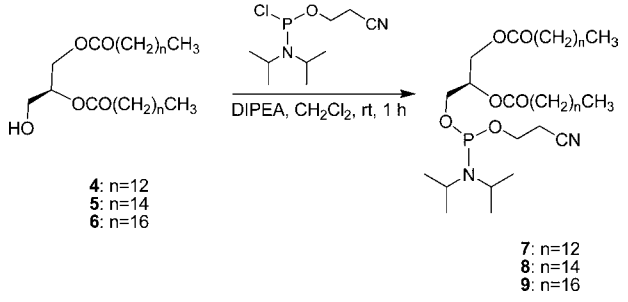

4: n=12
5: n=14
6: n=16

7: n=12
8: n=14
9: n=16

Once the building blocks needed to perform the planned synthesis were available, its actual feasibility was verified by performing the synthesis of some phosphatidyl derivatives of the tetradecamer 5′-TGGCTTGAAGATGT-3′. The latter sequence was designed to bind to the 261−274 site of the human $VEGF_{165}$ mRNA coding region.[26]

The synthesis was performed on a commonly used automated DNA synthesizer, equipped with a column filled with the previously prepared DMT-T-loaded support **3**. The followed protocol (Scheme 4) was the same as in the current solid-phase synthesis of oligodeoxynucleotides except that HOBt was used as the activator and no capping treatment was performed throughout the synthesis.

Once the tetradecamer was elongated on the solid phase, the last coupling step was carried out by using the appropriate diacylglycerophosphoramidite (**7**, **8**, or **9**) in order to obtain 5′-*O*-(1,2-di-*O*-tetra-, 5′-*O*-(1,2-di-*O*-hexa-, or 5′-*O*-(1,2-di-*O*-octadecanoyl-*sn*-glycero-3-*O*-phosphoryl)-TGGCTTGAAGATGT (**10**, **11**, or **12**, respectively). To increase coupling efficiency to as high as possible, this step was repeated twice. It should also be noted that anhydrous dichloromethane was used to dissolve the phosphoramidites **7**−**9**, these being practically insoluble in the most widely used acetonitrile. The final removal of phosphate protecting groups was accomplished by passing through the reaction column a solution of 1,8-diazabicyclo[5.4.0]undec-7-ene (DBU) in acetonitrile,[27] while each of the synthesized PODNs (**10**−**12**) was detached from the solid support following a treatment with tetrabutylammonium fluoride (TBAF)/acetic acid.[21] The TBAF excess was next removed by ion-exchange chromatography.

HPLC analysis of the crude eluate showed, in each case, the synthesized PODN as the highest peak in the chromatogram. Subsequent semipreparative HPLC allowed us to obtain chromatographically pure **10**, **11**, and **12** in a final yield of 33%, 27%, and 31%, respectively (for quantification see Experimental Section). The retention times of the three PODNs on a C-8 reverse-phase HPLC column provided an approximate indication of their relative hydrophobicity (Figure 1). As expected, hydrophobicity increased in the following order: unmodified oligonucleotide < **10** < **11** < **12**.

ESI-MS(−) spectra of **10** or **11** showed major peaks corresponding, in both cases, to the relevant $[M - 3H]^{3-}$, $[M - 4H]^{4-}$, $[M - 5H]^{5-}$, $[M - 6H]^{6-}$, and $[M - 7H]^{7-}$ quasimolecular ions. In ESI-MS(−) spectrum of **12**, major peaks corresponded to $[M - 4H]^{4-}$, $[M - 5H]^{5-}$, $[M - 6H]^{6-}$, and $[M - 7H]^{7-}$ quasimolecular ions.

^{1}H NMR spectra of **10**, **11**, and **12**, performed in D_2O at room temperature, looked flattened and poorly resolved; this result was somewhat expected, given the strong tendency of these compounds to self-aggregate. When ^{1}H NMR experiments were carried out at 60 °C, more easily assignable spectra were obtained which were quite similar to each other. ^{1}H−^{1}H COSY experiments, also performed at 60 °C, supported most of the resonance assignments.

As an example, in the spectrum of **10** (Figure 2) the methyls of myristoyl chains gave a broad triplet at δ 0.95 ppm, the methylene envelope from γ- to μ-positions gave two signals at δ

dx.doi.org/10.1021/bc300602g | *Bioconjugate Chem.* 2013, 24, 648−657

Scheme 4. Synthesis of 5′-*O*-Phosphatidyl Conjugates of the Antisense Sequence TGGCTTGAAGATGT

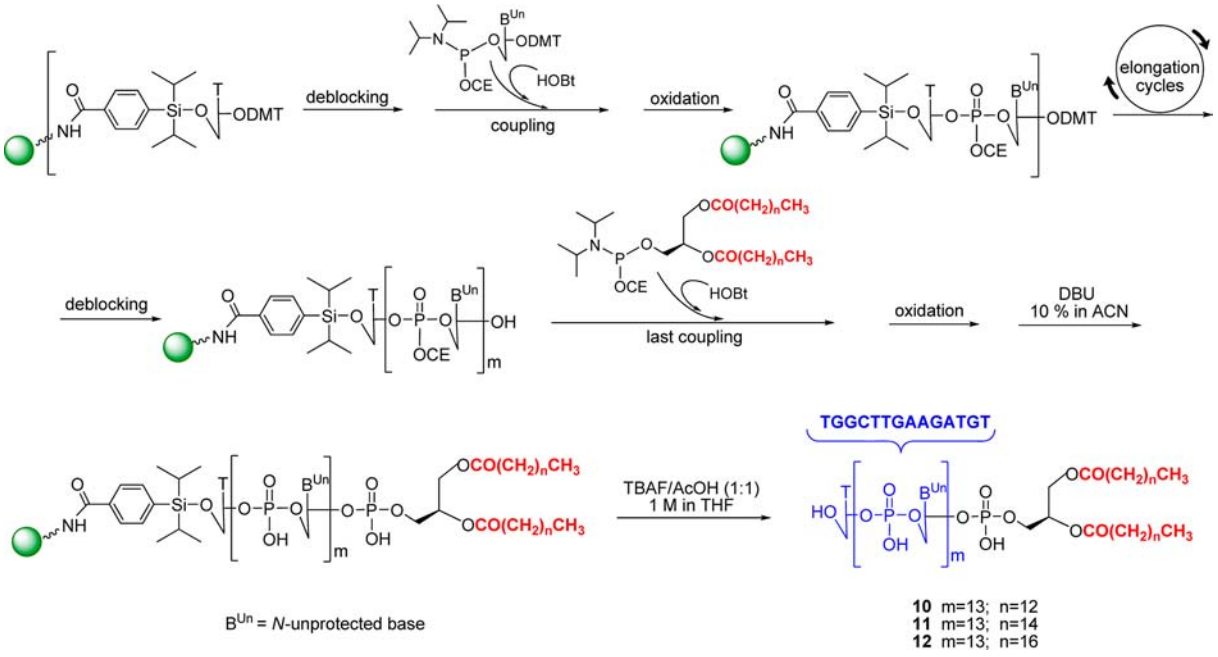

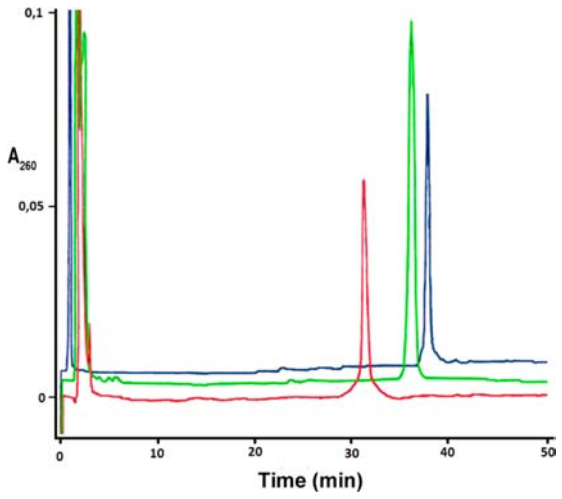

Figure 1. HPLC (RP-8 column) assessment of the relative hydrophobicities of PODNs: red, **10**; green, **11**; and blue, **12**. Hydrophobicity increased with the number of carbon atoms in the acyl chains as indicated by the increased retention time.

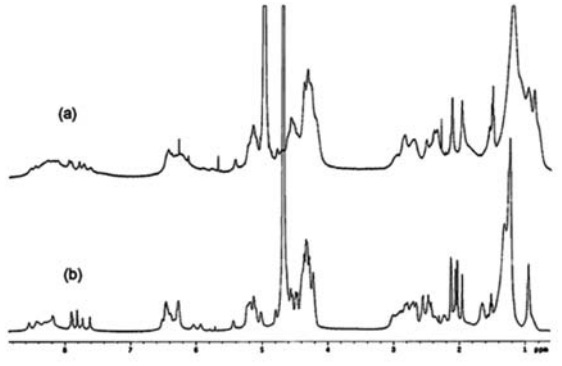

Figure 2. ^{1}H NMR spectrum of PODN **10** at 25 (a) and 60 °C (b) in D_2O.

1.22 and 1.31, and the two β-CH_2 appeared as a multiplet at δ 1.65; on the basis of the α-CH_2/β-CH_2 correlation peak present in the COSY spectrum, it was possible to assign the resonance of the two α-CH_2 at δ 2.47. The methyls of thymine T12, T14, and T1 gave signals at δ 1.95, 2.03, and 2.06 respectively, while those of T5 and T6 gave two partially overlapped signals at δ 2.12 and 2.13; the H-6 protons of T12, T1, and T14 appeared almost as singlets at δ 7.62, 7.73, and 7.81, respectively, while the H-6 of T6 and T5 appeared at δ 7.89 and 7.90 as two partially overlapped signals. These assignments were done on the basis of shielding effects on methyl or H-6 exerted by 5′-neighboring or 3′-neighboring purine, respectively,[28] and of the presence of the H-6/CH_3 cross peaks in the COSY spectrum. The resonances of H-2 and H-8 of adenines, H-8 of guanines, and H-6 of cytosine were present in the region at δ 8.10−8.60 (13 H altogether), while the signal of the H-5 of cytosine was superimposed on multiplets at δ 6.19−6.59 (13 H altogether) of most H-1′ protons of deoxyribose rings. The remaining H-1′ signals gave multiplets at δ 5.93 (1 H) and 6.04 (1 H). The resonances of H-3′ protons appeared as multiplets at δ 4.79 (1 H) and in the region at δ 4.79−5.28 (12 H); the resonance of the H-3′ of T14 was obscured by the residual HOD signal. H-5′, H-5″, and H-4′ of deoxyribose rings gave overlapped multiplets in the region at δ 4.15−4.63, altogether with H_2-3, H-1a, and H-1b of glycerol, whose H-2 appeared as a multiplet at δ 5.44. On the basis of the H-1a/H-2 and H_2-3/H-2 cross peaks in the COSY spectrum, it was possible to assign the resonances of the H_2-3 and H-1a protons of glycerol at δ 4.26 and 4.35, respectively. In the same COSY spectrum, it was not possible to observe the correlation between the H-1b and H-2 protons, probably due to the small value of their coupling constant.

Interaction of PODNs with a Lipid Bilayer. The desired ability of the synthesized PODNs to interact with cell membrane was investigated by quartz crystal microbalance with dissipation monitoring (QCM-D).[29] By these experiments, the extent to which each PODN was retained by a lipid bilayer consisting of palmitoyloleoylphosphatidylcholine (POPC) was

dx.doi.org/10.1021/bc300602g | *Bioconjugate Chem.* 2013, 24, 648−657

measured. Experiments were carried out on PODNs **10** and **11**, both showing an excellent affinity toward the bilayer. A more detailed analysis of these results, in order to clarify the way in which this interaction occurs, is currently in progress and will be addressed in a forthcoming publication.

Enzymatic Digestion of PODNs. Nuclease stability of the synthesized lipid−ODN was assayed in parallel experiments in which PODNs **10**−**12** and the relevant free ODN were subjected to enzymatic hydrolysis by snake venom phosphodiesterase. In the experimental conditions used, the hydrolysis of the free ODN was almost complete after 20 min, while at this same time PODNs **10**−**12** had suffered only near 17−30% degradation (Figure 3).

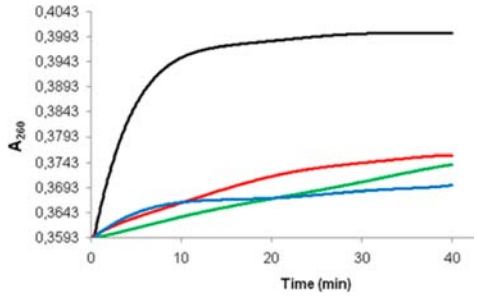

Figure 3. Snake venom phosphodiesterase degradation of free ODN (black) and the relevant PODN **10** (red), PODN **11** (green), and PODN **12** (blue). Oligonucleotides were incubated as described under Experimental Procedures. The progress of each reaction was monitored by determining the increase in the absorbance value at 260 nm.

Complete hydrolysis of the DNA backbone of PODNs **10**−**12** was assessed after 24 h of enzymatic digestion. For each of the three PODNs, HPLC/MS analysis of the final reaction mixture showed the presence of 5′-*O*-phosphatidylthymidine together with the four 5′-*O*-phosphoryl-nucleosides expected for the remaining part of the ODN sequence. It is interesting to note in this regard that phospholipase D has been reported to degrade 5′-*O*-phosphatidyl-nucleosides giving free nucleosides.[30] So, these results would be in line with the desired increased resistance to exonucleases of PODNs, as well as with their complete biodegradability. Bovine spleen phosphodiesterase had no effect on any PODNs **10**−**12**.

Finally, we considered that PODN molecules are phospholipid derivatives, and as such are potential substrates for phospholipases. So, PODN **10** was screened using phospholipase C and phospholipase D.[31] In the experiments, monitored by HPLC analysis, the lipid−DNA conjugate was found to remain intact using either phospholipase C or phospholipase D under standard conditions.

Duplex Formation of PODNs with Complementary ODN. In order to evaluate the ability of antisense PODNs **10**−**12** to form duplexes with their sense ODN (5′-ACATCTTCAAGCCA-3′), this sequence and that of the unmodified antisense ODN were synthesized as well. Duplex stability is strictly related to its thermal stability[32] which is currently expressed in terms of melting temperature (Tm). So, differential scanning calorimetry (DSC) was used to obtain, in parallel experiments, thermal profiles from duplexes formed by the free antisense ODN or each of the antisense PODNs **10**−**12** with the relevant sense ODN.

Typical DSC scans obtained from antisense ODN/sense ODN and antisense PODN/sense ODN duplexes are shown in Figure 4, along with their repeated scans. In particular, the

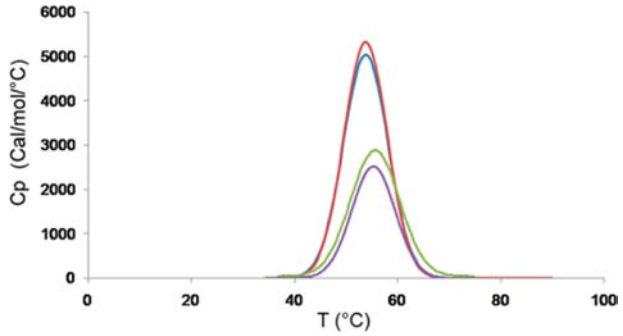

Figure 4. Overlapped DSC scans of unmodified antisense/sense duplex (red) and its rescan (blue); PODN **10**/ sense duplex (green) and its rescan (purple).

antisense PODN referred to in the figure is the 5′-*O*-(1,2-*O*-ditetradecanoyl-*sn*-glycero-3-*O*-phosphoryl)-tetradecamer **10**. The temperature of 55.9 °C corresponding to the peak maximum of the antisense PODN **10**/sense ODN duplex is a few degrees higher than that of the peak maximum of the unmodified antisense ODN/sense ODN duplex (54.3 °C), indicating that the former duplex is thermally stable at least as much as the corresponding antisense ODN/sense ODN duplex is. Also, the reappearance of the transition peaks upon a rescan of the samples shows that the transitions are reversible and there is no significant degradation of the sample after heating to 90 °C. The duplex from PODN **11** showed a quite similar behavior (Tm = 53.2 °C). The Tm value of PODN **12**/sense ODN duplex was by 9.1 °C lower than that of the reference unmodified duplex; this may probably be due to the larger size of the stearoyl chains in the phosphatidyl moiety, which somehow disturb the pairing of the bases close to them. It would be interesting to investigate further in this respect.

Antisense Activity of PODNs. Finally, considering that the sequence of the antisense oligonucleotide moiety of PODNs **10**−**12** had been designed to target at 261−274 of human $VEGF_{165}$ mRNA coding region, experiments were carried out to determine the ability of these lipid−ODN conjugates to elicit antisense effect in cells.

$VEGF_{165}$ is commonly expressed in a wide variety of human and animal tumors.[33] We assayed the ability of our antisense PODNs to turn down the VEGF mRNA expression in human SH-SY5Y neuroblastoma cells;[34] this would provide experimental foundation for possible future clinical application of these compounds.

In this regard, wanting to assay the antisense activity in experimental conditions of maximum VEGF expression by the cells, we evaluated the possibility of carrying out the tests on cell cultures treated with cobalt chloride ($CoCl_2$) which is known to produce cellular hypoxia,[35,36] which in turn induces VEGF production. For this purpose, the cellular response (in terms of VEGF mRNA production) to the treatment with different concentrations of $CoCl_2$ was investigated on neuroblastoma SH-SY5Y cells, the best results being obtained following administration of 25 μM $CoCl_2$.

Cells were then incubated, in parallel experiments, with **10**, **11**, or the relevant unmodified antisense ODN, each at various concentrations but, in any case, in the presence of 25 μM

dx.doi.org/10.1021/bc300602g | *Bioconjugate Chem.* 2013, 24, 648−657

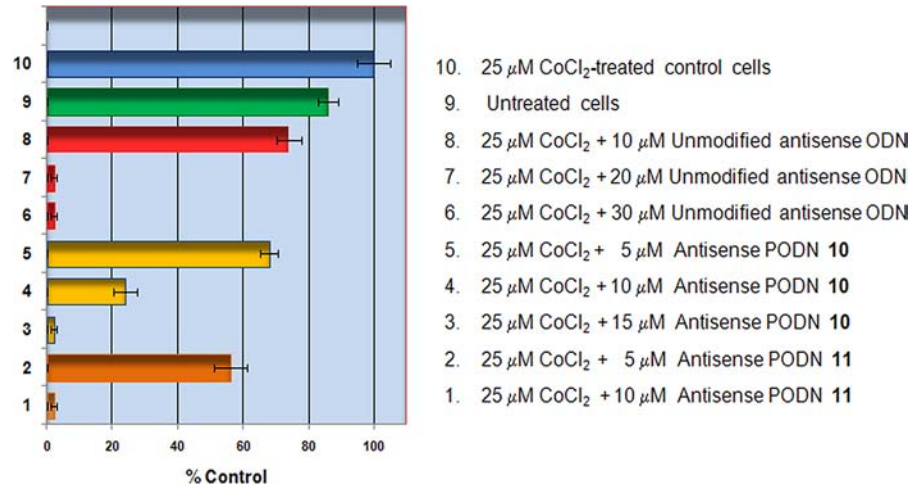

Figure 5. Effect of antisense PODNs **10** and **11** on VEGF-RNA expression in Neuroblastoma cells. The data are expressed as percentage to 25 μM $CoCl_2$-treated control cells. Results are presented as mean values with the corresponding standard deviation of three independent assays.

$CoCl_2$. After 60 h incubation, cells were treated with TRIzol reagent and mRNA was extracted (see Experimental Procedures). Transcription from mRNA to cDNA and PCR was then performed and the amplified cDNA was electrophoretically analyzed on agarose gel.

As can be deduced from the histogram reported in Figure 5, the unmodified antisense ODN was able to lower the cellular VEGF mRNA only if administered at concentrations equal to or greater than 20 μM. Both PODNs **10** and **11** produced, however, a significant lowering of the target mRNA already at 10 μM concentration. All the experiments were accompanied by analogous and parallel experiments aimed at assessing cell viability in the various experimental conditions. It is interesting to note that cell viability test (MTT) showed (see Figure S1 under Supporting Information) a mild cellular suffering only in the case of the administration of 20−30 μM free ODN.

When the above-discussed ability of PODNs to interact with lipid bilayers is taken into account, these results could be attributed, at least partly, to an increased cellular uptake of these compounds as compared with the unmodified antisense ODN. However, the improved resistance of PODNs to degradation by nucleases may also having a role in determining the extent of their antisense activity. That the findings may be due to both factors cannot be excluded. Further studies are ongoing in this regard.

■ ASSOCIATED CONTENT

Supporting Information

^{1}H NMR spectra of compounds **1**, **2**, **8**, and **9**. Results of MTT test, Figure S1. This material is available free of charge via the Internet at http://pubs.acs.org.

■ AUTHOR INFORMATION

Corresponding Author

*Phone +39 095 7385022. Fax +39 095 580138. E-mail: valentina.greco@ibb.cnr.it.

Notes

The authors declare no competing financial interest.

■ ACKNOWLEDGMENTS

The authors are grateful to Prof. C. La Rosa for letting use of the microDSC instrument and to Prof. C. Satriano for having carried out the measurements on the QCM-D instrument. This work was financially supported by Università degli Studi di Catania (PRA), Catania, Italy.

■ ABBREVIATIONS

ODN, oligodeoxynucleotide; VEGF, vascular endothelial growth factor; ASONs, antisense oligonucleotides; 5′-GPODNs, 5′-*O*-glycerophosphoryloligonucleotides; Ly-PODNs, lysophosphatidyloligonucleotides; HOBt, 1-hydroxybenzotriazole; PODN, phosphatidyloligodeoxynucleotide; CPG, controlled pore glass; HCP, highly cross-linked polystyrene; LCAA-CPG, long chain aminoalkyl-CPG; DMT-T, 5′-*O*-(4,4′-dimethoxytrityl)thymidine; DBU, 1,8-diazabicyclo[5.4.0]undec-7-ene; TBAF, tetrabutylammonium fluoride; QCM-D, quartz crystal microbalance with dissipation monitoring; POPC, palmitoyloleoylphosphatidylcholine; DSC, differential scanning calorimetry; PCR, polymerase chain reaction; MTT, 3-(4,5-dimethylthiazol-2-yl)-2,5-diphenyltetrazolium bromide

■ REFERENCES

(1) Crooke, S. T. (1995) Delivery of oligonucleotides and polynucleotides. *J. Drug Target 3*, 185−190.

(2) Stein, C. A., and Narayan, R. (1996) Antisense oligodeoxynucleotides: internalization, compartmentalization and nonsequence specificity. *Perspect. Drug Discovery 4*, 41−50.

(3) Bichenkov, E. E., Budker, V. G., Zarytova, V. F., Ivanova, E. M., Lokhov, S. G., Savchenko, E. V., and Teplova, N. M. (1988) Interaction of cholesterol-modified polynucleotide with phosphatidylcholine liposomes. *Biol. Membr. 5*, 735−742.

(4) Boutorin, A. S., Gus'kova, L. V., Ivanova, E. M., Kobetz, N. D., Zarytova, V. F., Ryte, A. S., Yurchenko, L. V., and Vlassov, V. V. (1989) Synthesis of alkylating oligonucleotide derivatives containing cholesterol or phenazinium residues at their 3′-terminus and their interaction with DNA within mammalian cells. *FEBS Lett. 254*, 129−132.

(5) Letsinger, R. L., Alul, R. A., Farooqui, F., Gryaznov, S. M., and Kinstler, O. (1991) Synthesis and properties of modified oligonucleotides. *Nucleic Acids Symp. Ser. 24*, 75−78.

(6) Krieg, A. M., Tonkinson, J., Matson, S., Zhao, Q., Saxon, M., Zhang, L. M., Bhanja, U., Yakubov, L., and Stein, C. A. (1993) Modification of antisense phosphodiester oligodeoxynucleotides by a 5′ cholesteryl moiety increases cellular association and improves efficacy. *Proc. Natl. Acad. Sci. U. S. A. 90*, 1048−1052.

(7) MacKellar, C., Graham, D., Will, D. W., Burgess, S., and Brown, T. (1992) Synthesis and physical properties of anti-HIV antisense oligonucleotides bearing terminal lipophilic groups. *Nucleic Acids Res. 20*, 3411−3417.
(8) Manoharan, M., Tivel, K. L., and Cook, P. D. (1995) Lipidic nucleic acids. *Tetrahedron Lett. 36*, 3651−3654.
(9) Tomkins, J. M., Barnes, K. J., Blacker, A. J., Watkins, W. J., and Abell, C. (1997) Lipophilic modification of oligonucleotides. *Tetrahedron Lett. 38*, 691−694.
(10) Shea, R. G., Marsters, J. C., and Bischofberger, N. (1990) Synthesis, hybridization properties and antiviral activity of lipid-oligodeoxynucleotide conjugates. *Nucleic Acids Res. 18*, 3777−3783.
(11) Lorenz, C., Hadwiger, P., John, M., Vornlocher, H. P., and Unverzagt, C. (2004) Steroid and lipid conjugates of siRNAs to enhance cellular uptake and gene silencing in liver cells. *Bioorg. Med. Chem. Lett. 14*, 4975−4977.
(12) Gissot, A., Camplo, M., Grinstaff, M. W., and Barthélémy, P. (2008) Nucleoside, nucleotide and oligonucleotide based amphiphiles: A successful marriage of nucleic acids with lipids. *Org. Biomol. Chem. 6*, 1324−1333.
(13) Pfeiffer, I., and Hook, F. (2004) Bivalent cholesterol-based coupling of oligonucleotides to lipid membrane assemblies. *J. Am. Chem. Soc. 126*, 10224−10225.
(14) Yoshina-Ishii, C., Miller, G. P., Kraft, M. L., Kool, E. T., and Boxer, S. G. (2005) General method for modification of liposomes for encoded assembly on supported bilayers. *J. Am. Chem. Soc. 127*, 1356−1357.
(15) Rabuka, D., Forstner, M. B., Groves, J. T., and Bertozzi, C. R. (2008) Non-covalent cell surface engineering: incorporation of bioactive synthetic glycopolymers into cellular membranes. *J. Am. Chem. Soc. 130*, 5947−5953.
(16) Lonnberg, H. (2009) Solid-phase synthesis of oligonucleotide conjugates useful for delivery and targeting of potential nucleic acid therapeutics. *Bioconjugate Chem. 20*, 1065−1094.
(17) Chillemi, R., Aleo, D., Granata, G., and Sciuto, S. (2006) Synthesis of very short chain lysophosphatidyloligodeoxynucleotides. *Bioconjugate Chem. 17*, 1022−1029.
(18) Chillemi, R., Russo, D., and Sciuto, S. (1998) Chemoenzymatic synthesis of lysophosphatidylnucleosides. *J. Org. Chem. 63*, 3224−3229.
(19) Ohkubo, A., Ezawa, Y., Seio, K., and Sekine, M. (2004) *O*-selectivity and utility of phosphorylation mediated by phosphite triester intermediates in the *N*-unprotected phosphoramidite method. *J. Am. Chem. Soc. 126*, 10884−10896.
(20) Ohkubo, A., Seio, K., and Sekine, M. (2004) A new strategy for the synthesis of oligodeoxynucleotides directed toward perfect *O*-selective internucleotidic bond formation without base protection. *Tetrahedron Lett. 45*, 363−366.
(21) Kobori, A., Miyata, K., Ushioda, M., Seio, K., and Sekine, M. (2002) A new silyl ether-type linker useful for the automated synthesis of oligonucleotides having base-labile protective groups. *Chem. Lett. 31*, 16−17.
(22) Ohkubo, A., Sakamoto, K., Miyata, K., Taguchi, H., Seio, K., and Sekine, M. (2005) Convenient synthesis of *N*-unprotected deoxynucleoside 3′-phosphoramidite building blocks by selective deacylation of *N*-acylated species and their facile conversion to other *N*-functionalized derivatives. *Org. Lett. 7*, 5389−5392.
(23) SantaLucia, J. J. (1998) A unified view of polymer, dumbbell, and oligonucleotide DNA nearest-neighbor thermodynamics. *Proc. Natl. Acad. Sci. U.S.A. 95*, 1460−1465.
(24) Richter, R. P., Berat, R., and Brisson, A. R. (2006) Formation of solid-supported lipid bilayers: an integrated view. *Langmuir 22*, 3497−3505.
(25) Mosmann, T. (1983) Rapid colorimetric assay for cellular growth and survival − application to proliferation and cytotoxicity assays. *J. Immunol. Methods 65*, 55−63.
(26) Masood, R., Cai, J., Zheng, T., Smith, D. L., Naidu, Y., and Gill, P. S. (1997) Vascular endothelial growth factor/vascular permeability factor is an autocrine growth factor for AIDS-Kaposi sarcoma. *Proc. Natl. Acad. Sci. U.S.A. 94*, 979−984.
(27) Hogrefe, R. I., McCaffrey, A. P., Borozdina, L. U., McCampbell, E. S., and Vaghefi, M. M. (1993) Effect of excess water on the desilylation of oligoribonucleotides using tetrabutylammonium fluoride. *Nucleic Acids Res. 21*, 4739−4741.
(28) Mellema, J. R., Jellema, A. K., Haasnoot, C. A., Van Boom, J. H., and Altona, C. (1984) Conformational analysis of the single-helical DNA fragment d(T-A-A-T) in aqueous solution. The combined use of NMR proton chemical shifts and coupling constants obtained at 300 and 500 MHz. *Eur. J. Biochem. 141*, 165−175.
(29) Gambinossi, F., Banchelli, M., Durand, A., Berti, D., Brown, T., Caminati, G., and Baglioni, P. (2010) Modulation of density and orientation of amphiphilic DNA anchored to phospholipid membranes. I. Supported lipid bilayers. *J. Phys. Chem. B 114*, 7338−7347.
(30) Novozhilova, T. I., Malekin, S. I., Kozhukhov, V. I., Kruglyak, Yu. L., and Kurochkin, V. K. (2000) The phospholipase-induced degradation of phosphatidylnucleosides. *Russ. J. Bioorg. Chem. 26*, 213−215.
(31) Dennis, E. A. (1983) *Phospholipases*, The Enzymes (Boyer, P., Ed.) pp 307−353, Vol. *16* , Academic Press, Inc., New York.
(32) Chakrabarti, M. C., and Schwarz, F. P. (1996) Thermal stability of PNA/DNA and DNA/DNA duplexes by differential scanning calorimetry. *Nucleic Acids Res. 27*, 4801−4806.
(33) Hanahan, D., and Folkman, J. (1996) Patterns and emerging mechanisms of the angiogenic switch during tumorigenesis. *Cell 86*, 353−364.
(34) Meister, B., Grünebach, F., Bautz, F., Brugger, W., Fink, F.-M., Kans, L., and Möhle, R. (1999) Expression of VEGF and its receptors in human neuroblastoma. *Eur. J. Cancer 35*, 445−449.
(35) Liu, X. H., Kirschenbaum, A., Yao, S., Stearns, M. E., Holland, J. F., Claffey, K., and Levine, A. C. (1999) Upregulation of vascular endothelial growth factor by cobalt chloride-simulated hypoxia is mediated by persistent induction of cyclooxygenase-2 in a metastatic human prostate cancer cell line. *Clin. Exp. Metastasis 17*, 687−694.
(36) Kee, H. J., Koh, J. T., Kim, M. Y., Ahn, K. Y., Kim, J. K., Bae, C. S., Park, S. S., and Kim, K. K. (2002) Expression of brain-specific angiogenesis inhibitor 2 (BAI2) in normal and ischemic brain: involvement of BAI2 in the ischemia-induced brain angiogenesis. *J. Cereb. Blood Flow Metab. 22*, 1054−1067.